Painting-Type Passive Loose-Bolt Sensing Based on Abnormality-Induced Changes in Waveguide Resonance

Eri Matsunaga, Tadashi Minotani, *Member, IEEE*, and Masayuki Tsuda

***Abstract*—The ability to detect abnormalities in infrastructure automatically and remotely with a small number of sensors would greatly contribute to efficient and timely infrastructure inspection. Here, we propose a passive sensor that can be installed by painting. The painted waveguide-based sensor detects abnormalities in infrastructure from abnormality-induced changes in the resonance frequency of electromagnetic waves resonating inside the sensor. In this paper, the principle of detecting loose bolts with the painted waveguide-based sensor is demonstrated by simulation and experiment. The sensor is designed and fabricated as a resonator with resonance frequencies from 100 kHz to 2.5 GHz, which includes the UHF radio-frequency identification band, and the measurement frequency was set within this range. The fabricated sensor is capable of detecting not only a single loose bolt but also two or more loose bolts on the waveguide of the sensor to monitor.**

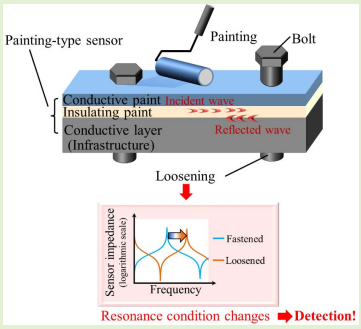

***Index Terms*— Electromagnetic wave, resonance, painting, waveguide, loose bolt, infrastructure.**

I. Introduction

IN RECENT years, infrastructure degradation has become a problem in developed countries. In Japan, many types of infrastructure constructed during the period of rapid economic growth in the 1950s through the 1970s are approaching the end of their average usage period [1]. Infrastructure is regularly inspected visually and in hammering tests [2], [3]. For example, cracks in bridges are detected visually as cracks in painted film accompanied by rust water, and then conducting nondestructive testing, mainly with penetrants [4]. To check for loosened bolts, visual inspections using markings or axial force measurements using ultrasonic waves are performed [5], [6]. However, the determination of abnormalities in the initial stage largely depends on the experience of the inspector [7], and facility inspections are costly and labor-intensive because inspectors have to bring measurement instruments and other equipment to the site for individual inspections. In addition, infrastructure may have complicated and diverse shapes with many blind areas or may be located in high places, making them difficult to access and inspect on a regular basis. Therefore, there is a great need for the ability to monitor the conditions of infrastructure by using sensors [8], [9].

Small cracks and loose bolts can lead to major accidents, such as bridge collapses [10], [11]. In particular, inspection for the loosening of bolts, which occurs due to repeated loads and vibrations, is important because a huge number of bolts are often installed at joints. Sensors to detect bolt loosening have been demonstrated, which have used tension indicator methods with a special washer put under the bolt head or nut [12], [13], methods based on piezoelectric elements [14], [15], and image processing [16], [17]. Although the sensitivities of these sensors are high, there are some issues in using them in practice. Sensors designed for detecting a loose bolt must be installed for each bolt, so the number of sensors will be huge [12]–[15]. Although image-processing systems can detect multiple bolts simultaneously, they require lighting, a suitable environment for installing a camera, and a power supply. Moreover, image-processing systems are not suitable for use in blind areas or buried environments [18]. For sensors to be practical, they should be low cost and able to be installed in small numbers and still be effective. Moreover, they should able to use wireless from an accessible location [19]. As well, their operational costs once they have been installed, i.e., the costs of replacing their electronic boards, active electronics and batteries, have to be low [20]. The need for extensive coverage also requires the sensors to follow the shape of complex infrastructure components.

Manuscript received July 23, 2021; accepted August 5, 2021. Date of publication August 9, 2021; date of current version October 1, 2021. The associate editor coordinating the review of this article and approving it for publication was Dr. Cheng-Ta Chiang. *(Corresponding author: Eri Matsunaga.)*

The authors are with NTT Device Technology Laboratories, NTT Corporation, Kanagawa 243-0198, Japan (e-mail: eri.matsunaga.ht@hco.ntt.co.jp).

Digital Object Identifier 10.1109/JSEN.2021.3103380

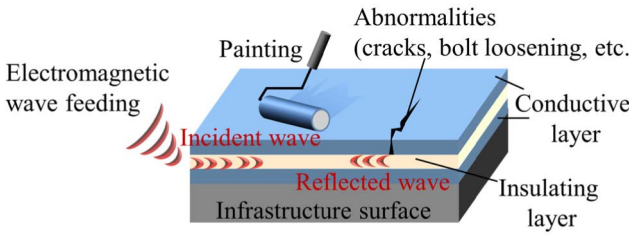

Fig. 1. Basic structure of painting type sensor based on waveguide.

We have developed a paintable wireless passive sensor based on a waveguide that does not require batteries, which can be easily applied by simply painting along an arbitrary surface shape [21]. We previously demonstrated that cracks can be detected by changing the resonance frequency of the sensor's electromagnetic waves. To detect abnormalities without batteries and active electronics, we have also demonstrated that sensor works as a paintable wireless passive sensor [22]. The sensor has an antenna made of the same kind of paint to supply wireless power from external equipment to the sensor.

In this paper, we focus on inspection of bolts collectively installed in a joint and develop a sensor structure can detect loosening of multiple bolts with a single sensor element. With the aim of achieving the same level of detection accuracy as conventional visual inspection and image-processing technology, we have proposed a sensor principle for detecting the looseness of one bolt, demonstrated the detection, and evaluated the sensitivity [22]. In this study, we apply its detection principle to a single sensor element capable of detecting the looseness of a plurality of bolts and demonstrate its operation.

II. Theory and Design Concept of Painting-Type Sensor

A. Basic Structure of the Sensor

Figure 1 shows the basic structure of the painting-type sensor based on a waveguide. The sensor can be easily applied by simply painting the surface of an object. It can be applied to equipment with complex shapes and many bolts, such as infrastructure equipment. It can also be applied with a machine, such as a printer [23], [24], or can be applied directly with a spatula in the field where a printer is not available. The basic structure of the sensor is a transmission line (parallel plate waveguide) consisting of a three-layer structure in which an insulating layer through which electromagnetic waves propagate is sandwiched between upper and lower conductive layers. By using electromagnetic waves, i.e., high-frequency waves, a parallel plate waveguide structure can be used for wireless inputting and outputting of electromagnetic waves and sensing of multiple types of abnormality. The conductive layers confine electromagnetic waves in the insulating layer and eliminate the effects of contamination, such as dust adhesion to the sensor surface. If the infrastructure is composed a conductive material, the lower conductive layer can be omitted because the surface of the infrastructure plays that role. In that case, the sensor consists of two layers. Electromagnetic waves propagate into the sensor from the outside wirelessly or through a wired connection, and the reflected waves are observed. When an abnormality such as a loose bolt or a crack occurs, the position of the reflection point of the electromagnetic wave and the reflection path change, and the abnormality can be detected.

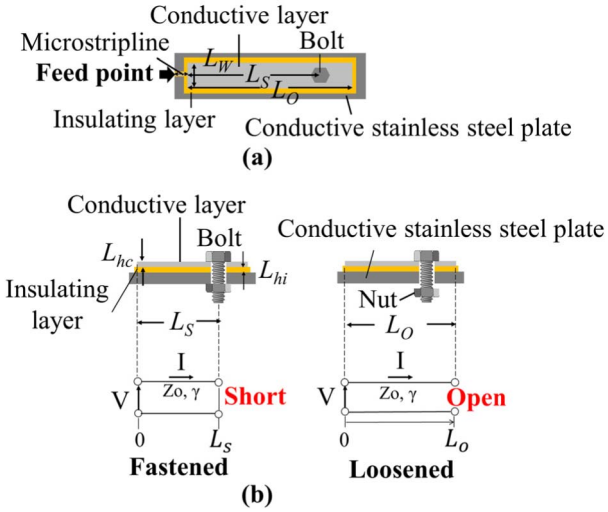

Fig. 2. Sensor structure for detection of a single loose bolt. (a) Top view. (b) Cross-sectional view. The bottom left and bottom right images show the fastened and loosened bolt and the corresponding equivalent circuits.

B. Sensor Design for Detecting a Single Loose Bolt

Figure 2 shows the sensor structure for detecting of a single loose bolt. From the left side of the sensor, a high-frequency electromagnetic wave is introduced through a microstrip line (MSL) [25], [26]. At the right side of the sensor (length of L_s from sensors left edge), a conductive bolt is fastened through a via hole. The size of the hole is larger than the diameter of the bolt thread so that the side surface of the bolt thread and the end face of the hole of the conductive layers do not come into electrical contact with each other. When the bolt is fastened, electrical contact between upper and bottom conductive layer is established through the bolt head and nut. This is defined as the normal initial state. If the bolt is loosened, electrical contact between the upper and bottom layer is broken. When the resistance component of the transmission line is negligible and the contact point between the MSL and the waveguide structure is defined as the sending end, the equivalent circuits in the case of a fastened and loosened bolt are shown in the lower part of Fig. 2. The sensor impedance when the bolt is fastened and loosened are given by

$$Z = Z_0 \tanh \gamma L_s \tag{1}$$

and

$$Z = Z_0 \coth \gamma L_o \tag{2}$$

respectively [27], where Z is sensor impedance, Z_o is characteristic impedance, γ is the propagation constant, and L_o is the total length of the sensor structure. The frequency response when the bolt is fastened is determined by L_s. Because the sensor is electrically closed at the location of the bolt defined

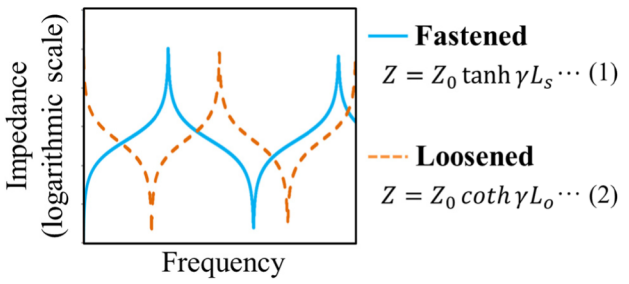

Fig. 3. Conceptual diagram of the frequency characteristics of the sensor impedance based on the equivalent circuit.

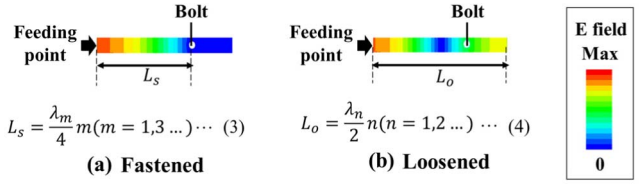

Fig. 4. Top view of electric field distribution (m = n = 1) in the insulating layer and resonance conditions.

by L_s becomes a resonance node. Resonance condition when Z becomes infinite is given by

$$L_s = \frac{\lambda_m}{4} m \quad (m = 1, 3 \ldots) \tag{3}$$

where m is an odd number, and λ_m is the mth mode's wavelength in the medium. The resonance occurs when L_s is an odd multiple of $\lambda_m/4$.

On the other hand, when the bolt is loosened, the right end of the sensor is electrically open because the electrical short circuit between the upper and lower conductive layers is lost. The frequency response when the bolt is loosened is determined by L_o. The resonance condition when Z becomes infinite is given by

$$L_o = \frac{\lambda_n}{2} n \quad (n = 1, 2 \ldots) \tag{4}$$

where n is natural number, and λ_n is the n th mode's wavelength in the medium. Resonance occurs when L_o is an integral multiple of $\lambda_n/2$, that is, when the effective length of the sensor changes from L_s to L_o.

As described above, the resonance condition changes due to the change in electrical conduction between the conductive layers depending on the fastening and loosening of the bolt, and the resonance frequency is determined. A conceptual diagram of the frequency characteristics of the sensor impedance based on the equivalent circuits is shown in Fig. 3, and the electric field distribution (m = n = 1) in the insulating layer and the resonance condition of the circuit model, obtained by electromagnetic field simulation, are shown in Fig. 4. The electromagnetic field simulation was performed using HFSS Electromagnetic version 20.1. The hybrid finite-element boundary integral method with both the finite element method and an integral equation was used to handle the large-scale calculations more accurately in less simulation time [28]. The simulation results suggest that the proposed design can detect loose bolts by using changes in the resonance frequency.

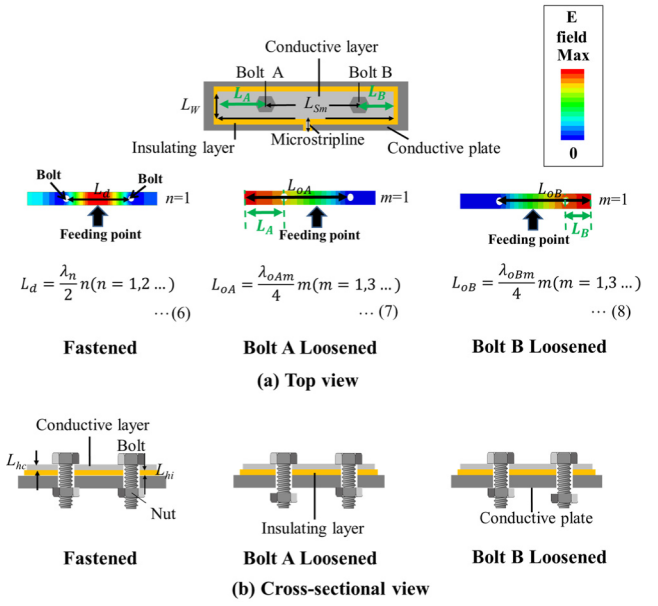

Fig. 5. Sensor structure for identifying a loose bolt among multiple bolts. (a) Top view of the sensor structure and the electric field distribution ($m = n = 1$) in the insulating layer. (b) Cross-sectional view of the sensor.

As for detection of a single loose bolt, as shown in Fig. 3, if the bolt or nut is completely separated from the conductive layer and the electrical contact between the conductive layers is broken, and it is possible to detect bolt loosening even with direct current (DC) or near-DC. However, as we will show in section IV, the detection sensitivity of near-DC for a single loose bolt is inferior to that of detection at high frequency and a loose bolt among multiple bolts cannot be detected with DC or near-DC.

C. Sensor Design for Identifying a Loose Bolt Among Multiple Bolts

To detect a single loose bolt, an electromagnetic wave is fed from the end of the sensor to a bolt installed on the opposite side as shown in Fig. 2. When the bolt is fastened, the resonance frequency is determined by the distance between the feeding point and the bolt. When the bolt is loosened, the frequency response changes, and the resonance frequency is determined by the entire quasi-one-dimensional sensor length, namely the total of the length from the feed point to the bolt and the extra length (the length between each bolt and the end of the sensor opposite the feed point). To monitor multiple bolts with a single feeding point, the number of quasi-one-dimensional waveguides increases with the number of bolts from the feed point. To identify the loose bolt among multiple bolts, the extra length should be changed. This allows us to design a sensor that can distinguish and detect the loosening of multiple bolts from a single feeding point.

Fig. 5 shows the sensor structure for demonstrating how the sensor can be used to identify a loose bolt among multiple bolts. The MSL is located between the bolts, and it is designed so that the extra lengths of each bolt are different:

$$L_A \neq L_B \tag{5}$$

L_A is the extra length between the left bolt A and the left edge of the sensor, L_B is extra length between the right

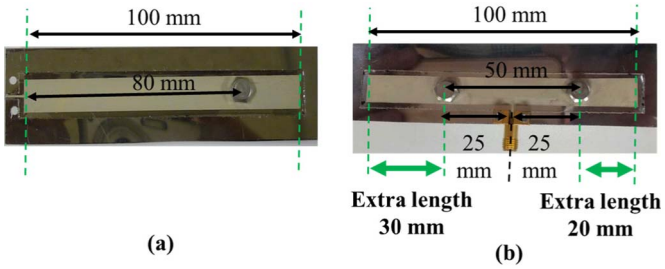

Fig. 6. Appearance of fabricated sensors. (a) Sensor with single bolt installed (see Fig. 2 for the structure). (b) Sensor with multiple bolts installed (see Fig. 5 for the structure).

bolt B and the right edge of the sensor. When the two bolts are fastened, a resonance condition is established where the electric field intensity is zero at the positions of bolt A and bolt B. The resonance condition is given by

$$L_d = \frac{\lambda_{sn}}{2} n \quad (n = 1, 2 \ldots) \tag{6}$$

where L_d is the distance between bolt A and bolt B, n is a natural number, λ_{sn} is the nth mode's wavelength in the medium when the two bolts are fastened.

On the other hand, when bolt A is loosened, the electric field intensity at its position has a finite value and resonates at length L_{oA}, which is the sum of L_d and the extra length L_A. The resonance condition is given by

$$L_{oA} = \frac{\lambda_{oAm}}{4} m \quad (m = 1, 3 \ldots) \tag{7}$$

where m is an odd number, and λ_{oAm} is the mth mode's wavelength in the medium when bolt A is loosened. Similarly, when bolt B is loosened, the resonance condition is given by

$$L_{oB} = \frac{\lambda_{oBm}}{4} m \quad (m = 1, 3 \ldots) \tag{8}$$

where L_{oB} is the sum of L_d and the extra length L_B, m is an odd number, and λ_{oBm} is the mth mode's wavelength in the medium when bolt B is loosened.

Fig. 5 also shows the results of an electromagnetic field simulation of the electric field distribution ($m = n = 1$) in the insulating layer and the resonance conditions in the circuit model. The resonance wavelengths of each mode are different for each bolt because the extra lengths of each bolt are different from each other, i.e.,

$$\lambda_{oAm} \neq \lambda_{oBm} \tag{9}$$

As described above, a loose bolt among two bolts (or among multiple bolts) can be identified by controlling the resonance frequency when the bolt is loosened using the difference in the extra length.

III. Fabrication and Experimental Setup

A. Fabricated Sensors

Figure 6 shows the appearance of the fabricated sensor. Stainless steel plates with a length of 120 mm, width of 30 mm, and thickness of 0.5 mm were prepared, and they correspond to infrastructure fixed with a bolt. Two sensor layers were applied by painting the top surface of the plate.

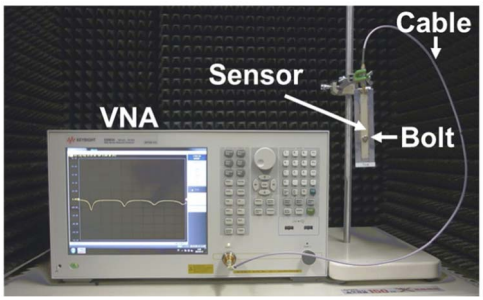

Fig. 7. Setup of frequency response measurement.

The top conductive layer consisted of commercially available conductive paint [29] that is composed of polyester resin containing silver powder and has conductivity of 1.4×10^6 S/m and a curing time of 3 hours at 25°C. The conductive paint layer was dried in a dryer set at 55°C for about 1 hour. The painted had a length L_o of 100 mm, width of 10 mm, and target thickness of 0.05 mm. The thickness of the conductive paint was evaluated at five points on each sensor. The average thickness for each sensor was 0.038 mm; we concluded that these thickness variations would have no effect if the paint is thicker than the skin depth. The lower layer was applied using a commercially available insulating paint composed of epoxy resin that has a dry tack time of 6 hours at 25°C and relative permittivity ε_r of 3.5 on the stainless steel plate. The insulating paint layer was dried in the dryer at 55°C for about 1 hour. The target thickness was 0.4 mm and the width and length were 4 mm larger than those of the conductive paint layer to prevent an electrical short circuit between the stainless steel plate and the conductive paint. The thickness of the insulating paint was evaluated at five points on each sensor, and the average thickness was 0.44 mm, with a maximum variation of ±30 % within all sensors. The entire length of the sensor, L_o, was designed to be almost the same as a half -wavelength in the medium in the ultra-high frequency (UHF) band, which is the fundamental wave when all the bolts in the sensor are loosened as shown in Fig. 6(a) or (b). In the sensor with a single bolt installed, an MSL with a length of 7 mm to feed the electromagnetic wave into the sensor was fabricated on one side of the sensor by using the same paints. L_s was designed to be 80 mm in order to observe the first- and third-order modes in the measurement frequency range. In the sensor with two bolts installed, L_{sn} was designed to be 50 mm, L_{oA} to be 80 mm (extra length was 30 mm), and L_{oB} to be 70 mm (extra length was 20 mm). An MSL with a length of 7 mm was fabricated just midway between the bolts. This is because the resonance frequency when the two bolts are fastened is designed to shift to the long wavelength side and the short wavelength side when each bolt is loosened in the range near the resonance frequency. This reduces false positives of identifying loose bolts when monitoring in a narrow frequency range.

B. Measurement and Evaluation

Figure 7 shows the setup of the frequency response measurement. A vector network analyzer (VNA, N5063A, Keysight) was used to input electromagnetic waves to the

sensor and detect the reflected waves to measure the frequency response of the sensor impedance (1-port measurement). A coaxial cable connected to the network analyzer was connected to the connector at the end of the MSL, and AC voltage was applied to generate and propagate electromagnetic waves in the insulating layer for the reflection measurement. Calibration was performed at the end of the coaxial cable. The measurement frequency was set from 100 kHz to 2.5 GHz, which includes the UHF radio-frequency identification (RFID) band. The sensor impedance (input impedance) was obtained from the reflected wave (reflection coefficient, S11) of the S-parameter [30] measured by the network analyzer:

$$Z = Z_0 \frac{(1 + S_{11})}{(1 - S_{11})} \tag{10}$$

To evaluate the frequency response of the sensors, bolts with a diameter of 5 mm (SUS M5 bolts) were used, and the S-parameters were measured by the network analyzer when the bolt was fastened and when it was completely loosened. The fastened state was measured when the bolts were torqued to 3.0 N · m, which is the standard value of the standard T series for M5 bolts. The standard T series is the general tightening torque applicable to SS, SC, and SUS with strength classifications of 4.6 to 6.8, and it is applied to ordinary bolts, unless otherwise specified [31]. The loosened state was measured when the distance between the nut and the plate corresponding to the structure was 6 mm, and the nut was completely separated from the plate.

To estimate the minimum detection angle of bolt loosening, we examined the change in the resonance frequency against the bolt-rotation angle. The bolts were fastened to 3 N·m and then loosened in 5-degree increments up to 90 degrees. The S-parameters were measured by the network analyzer at each bolt-rotation angle.

IV. Results and Discussion

A. Detection of a Single Loose Bolt

Fig. 8(a) and (b) show the simulated and measured frequency response of the impedance of the sensor shown in Fig. 6(a). The simulated frequency response could be reproduced according to (1) and (2) in Fig. 3 when the bolt is fastened and fully loosened, respectively. At the first-order resonance (m = 1) when the bolt was fastened, the impedance is maximal at 0.50 GHz. This corresponds to a frequency at which a quarter wavelength in the medium is Ls = 80 mm. At the first-order resonance (n = 1) when the bolt was loosened, the impedance was maximal at 0.74 GHz. This corresponds to the frequency at which a half wavelength in the medium is Lo = 100 mm. The measured frequency response results show good agreement with the simulated results. For the experimental impedance frequency response curves, the first-order resonance (m = n = 1) appeared at 0.47 GHz when the bolt was fastened and 0.77 GHz when it was loosened. The large difference in resonance frequency enables us to determine whether a bolt is loose or not. By the increasing measurement frequency, the impedance and resonance damping are increased. This is mainly because the conductive particles in the painted conductive layer are non-uniform and the actual conductivity is lower than the value used in the simulation.

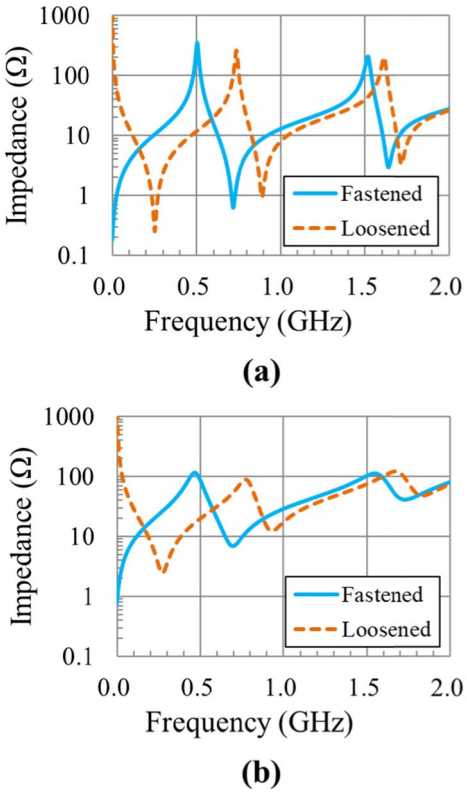

Fig. 8. Simulated and measured frequency response of sensor impedance when the bolt is installed at Ls = 80 mm. (a) Simulated result. (b) Measured results.

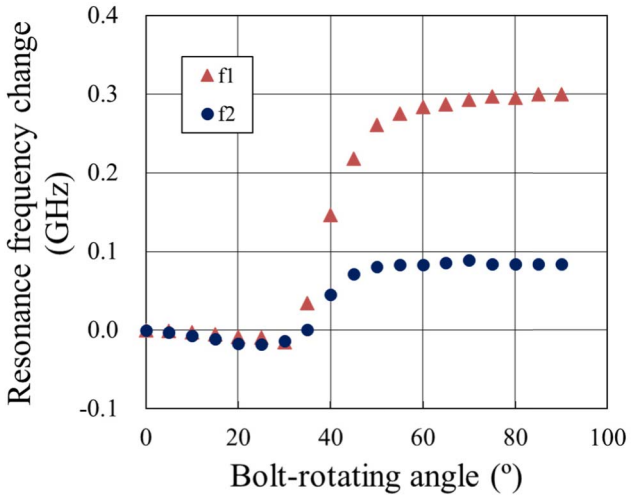

Fig. 9. Relationship between bolt rotating angle from fastened state and average resonance frequency change in three trials. The bolt was fastened at 3.0 N · m before loosening. f1 is the resonance peak of the lower-order mode ($m = n = 1$), and f2 is the resonance peak of the higher-order mode ($m = 3$, $n = 2$).

To estimate the minimum detection angle of the bolt, we examined the change in resonance frequency versus the bolt-rotation angle. As shown in Fig. 9, we calculated the average frequency change versus bolt-rotation angle in three trials of loosening a bolt fastened at 3.0 N · m (corresponding

to 0 degrees). We monitored the lower order mode (m = n = 1; named f1) and higher order mode (m = 3, n = 2; named f2). The f1 resonance frequency change from the state where the bolt is fastened to the state where it is loosened is larger than the f2. The f1 showed a clear frequency change at a bolt-rotating angle of 35°, while the f2 showed a gradual frequency change starting at around 40°. These conditions are roughly equivalent to a manual-fastening condition. The detection angle was also larger than in Ref. [16], where it was evaluated by using image-processing technology.

To consider the transition from the fastened state to a loosened one, we discuss the resonance condition in the case of a bolt that is not fully loosened. When electromagnetic waves are introduced at the incident point, the waves propagate to the reflection point and return to the incident point. At the reflection point, the phase of the wave rotates. The resonance condition of the electric field amplitude in the loosening process can be expressed by

$$k \cdot 2L + \theta = 2n\pi \tag{11}$$

where k is the wave number in the medium, L is the propagation distance of the electromagnetic wave from the incident to the reflection point, θ is the phase rotation angle at the reflection point, and n is a natural number.

From Eq. (11), we obtain

$$L = \left(\frac{n}{2} - \frac{\theta}{4\pi}\right)\lambda \tag{12}$$

where λ is the wavelength in the medium. When the bolt is fastened, the electric field is zero at the reflection point $L = L_s$, so the electromagnetic wave resonates with a fixed-end reflection ($\theta = \pi$). The same resonance condition as in (3) is obtained by substituting $\theta = \pi$, $L = L_s$, $n = m$, $\lambda = \lambda_m$ into (12). On the other hand, the electromagnetic wave resonates without phase rotation ($\theta = 0$) when the bolt is fully loosened. Here, the same resonance condition as in (4) is obtained by substituting $\theta = 0$, $L = L_o$, $\lambda = \lambda_n$ into (12). The change in resonance frequency caused by bolt rotation shown in Fig. 9 is described by (12), and the resonance frequency shifts to a shorter wavelength (higher frequency) during the bolt loosening process. When the wavelength is short relative to the total length of the sensor, the frequency change is also small; hence, so the displacement of the higher order modes is small.

To measure sensitivity accurately, difference in resonance frequency between when the bolt is fastened and completely loosened should be large. This is because the larger the difference is, the larger the frequency change in response to the loosening of the bolt becomes, and thus, the loosening of the bolt can be clearly determined. For this reason, it is better to use lower order modes with longer wavelengths, as shown in Fig. 9. In addition, the frequency difference is given by

$$f_{on} - f_{sm} = \frac{c}{\sqrt{\varepsilon_r}}\left(\frac{n}{2L_o} - \frac{m}{4Ls}\right) \tag{13}$$

where f_{on} is the resonance frequency in the nth mode when the bolt is loosened, f_{sm} is the resonance frequency in the mth mode when the bolt is fastened, and c is the speed of light in a vacuum. We consider, for example, a case where the modes under these experimental conditions (f1: $m = n = 1$ or f2: $m = 3$, $n = 2$) are substituted. In terms of the design of the present quasi-one- dimensional sensor, the bolt can be better installed closer to one of the ends of the sensor to increase the resonance frequency change.

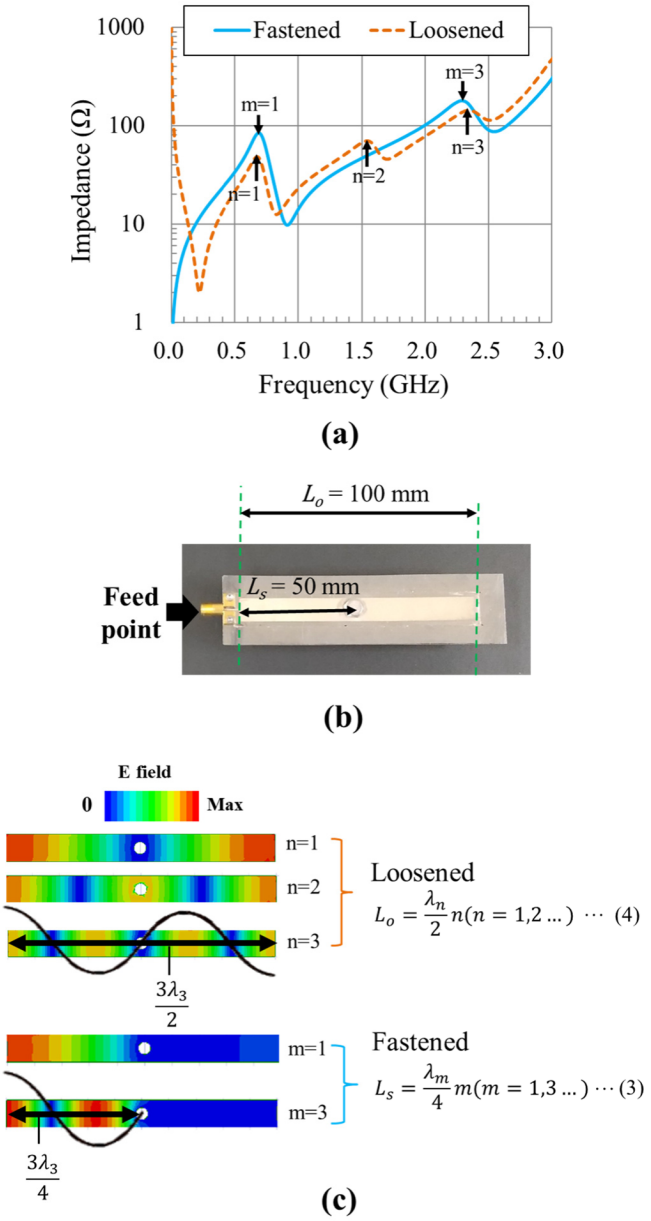

Fig. 10. Measured frequency response of sensor impedance when bolt is installed in the center of the sensor (L_S = 50 mm). (a) Measured results. (b) Sensor with single bolt installed and (c) top view of electric field distribution in the insulating layer in each resonance mode.

We also simulated and measured the sensor impedance with a bolt installed at the center of the sensor (L = 50 mm) as shown in Fig. 10. Resonance frequencies were almost the same when m and n were odd, because the electric field strength at the center of the sensor is zero when the bolt is fastened but also when it is loosened as shown in Fig. 10(b). That is, the sensor was unable to detect the loose bolt, because there was no difference in the resonance frequencies.

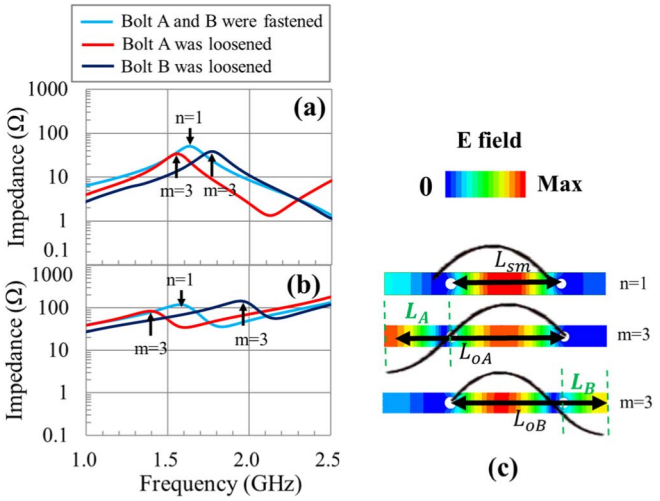

Fig. 11. Simulated (a) and measured (b) frequency response of impedance when sensor monitors multiple bolts. Bolt A (extra length was 20 mm) and B (extra length was 30 mm) were loosened from their fastened at 3.0 N · m. (c) Top view of electric field distribution in the insulating layer in each resonance mode.

On the other hand, focusing on the second mode (e.g., n = 2, resonance at one wavelength over the entire length of the sensor), which has the maximal electric field amplitude at the center of the sensor when the bolt is loosened, we see that the resonance peaks appeared only at the loosened bolt. The sensor can detect a loose bolt by the presence or absence of the resonance peak. Thus, when a bolt is installed at the center of the entire length of the sensor, only the peak of the resonance state when n is an even number can be used. It is obvious that it is better to install the bolt close to one end of the sensor rather than in the center. When the bolt is installed closer to the center of the sensor, the sensor needs to be designed keeping in mind that the modes that can be used are limited and that sensitivity will be reduced.

Finally, to evaluate the sensitivity by comparing measurements at low frequency (100 kHz), which are not affected by resonance like DC, with measurements at AC (alternating current above 0.1 GHz), a total of 24 sensors with a bolt installed at 10 mm to 90 mm from the edge of the sensor were fabricated and their sensor impedances were measured. At low frequency (100 kHz), the sensor impedance exceeded 50 Ω and the electrical contact was significantly reduced when the maximum bolt-rotating angle exceeded 80° for 24 sensors measurements. Under AC, the resonance frequency changed for all sensors when bolt-rotating angle exceeded at least 40°. This indicates that measurement under AC has better sensitivity than measurement under DC and has sufficient reproducibility.

B. Loose-Bolt Identification With Multiple Bolts Installed in Sensor

Fig. 11(a) and (b) show the simulated and measured frequency response of sensor impedance, when two bolts were installed in the sensor. For sensors with multiple bolts installed, the impedance does not change under DC or near DC until all the bolts are loosened, which makes it impossible to identify one loose bolt among multiple bolts installed in sensor, so sensor impedance should be monitored on a high-frequency band. We focused on a high-frequency band around 1.6 GHz, where both the $n = 1$ resonance frequency peak of the fastened bolts and $m = 3$ resonance frequency peak of the loosened bolt exist together in UHF band. This is because it is desirable to be able to detect and identify bolt loosening wirelessly with a single small antenna as a passive integrated sensor in the future. Although the measured impedance was higher than the simulated impedance, the behavior of the resonance frequency changes were in good agreement. The relatively higher measured impedance may be mainly due to the inhomogeneous distribution of conductivity in the conductive layer. It is considered that this can be improved by using a coating method with higher accuracy, for example, by mechanical coating with a coating machine.

When bolt A and B were fastened, the electric field strength became zero at the positions of the bolts. Therefore, the resonance condition in (6) was satisfied. When $n = 1$, the resonance length L_{sn} was $\lambda_{sn}/2 = 50$ mm, and the simulated and experimental resonance frequencies were 1.63 and 1.58 GHz, respectively. When bolt A was loosened, the resonance condition changed from that in (6) to that in (7). When $m = 3$, the resonance length L_{oA} was $\frac{3}{2}\lambda_{oAm} = 80$ mm, and the simulated and experimental resonance frequencies were 1.56 and 1.39 GHz, respectively. Similarly, when bolt B was loosened, the resonance condition in (8) was satisfied. When $m = 3$, the resonance length L_{oB} was $\frac{3}{2}\lambda_{oBm} = 70$ mm, and the simulated and experimental resonance frequencies were 1.77 and 1.95 GHz, respectively. When the bolt A was loosened, the peak shifted to the low- frequency side while both bolts were fastened. On the other hand, when bolt B was loosened, it shifted to the high- frequency side. As the sensor was designed to prevent false detection, we were able to successfully identify the loosened bolt by changing the extra length of each bolt even when multiple bolts were installed in the sensor. The sensor was designed so that the resonance frequency changes to both higher and shorter when each bolt is loosened from the fastened state. Compared to the case where both resonance frequencies shift to the same frequency side, the loosened bolt can be identified in the initial stage.

To estimate the minimum detection angle of the sensor, we examined the change in the resonance frequency against the bolt-rotation angle. Fig. 12(a) and (b) show the average frequency change in four trials of the resonance frequency responding to the bolt-rotation angle of bolt A and B from the initial state of fastening at 3.0 N·m. To identify a loose bolt in a narrow frequency range as mentioned above, we monitored the frequencies around 1.7 GHz. In the initial state (both bolts were fastened), the resonance frequency at the resonance condition $n = 1$ of (6) was observed. When the rotation angle of bolt A exceeded 30°, the resonance frequency shifted lower according to (7) with $m = 3$. During loosening of bolt B, it shifted higher according to (8) when the angle exceeded 30°. The minimum detection angles of bolt A and B were about the same even though the resonance wavelength frequency differed under the present conditions where the difference in the extra length to the resonance lengths was about 20%. In addition, this suggests the possibility of detection with

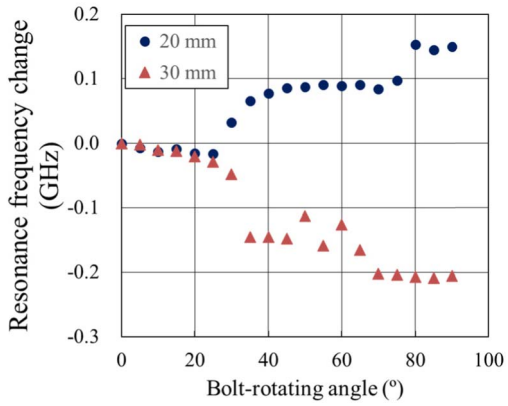

Fig. 12. Relationship between bolt rotating angle from fastened and average resonance frequency change in four trials. Bolt A (extra length was 20 mm) and B (extra length was 30 mm) were fastened at 3.0 N · m before loosening.

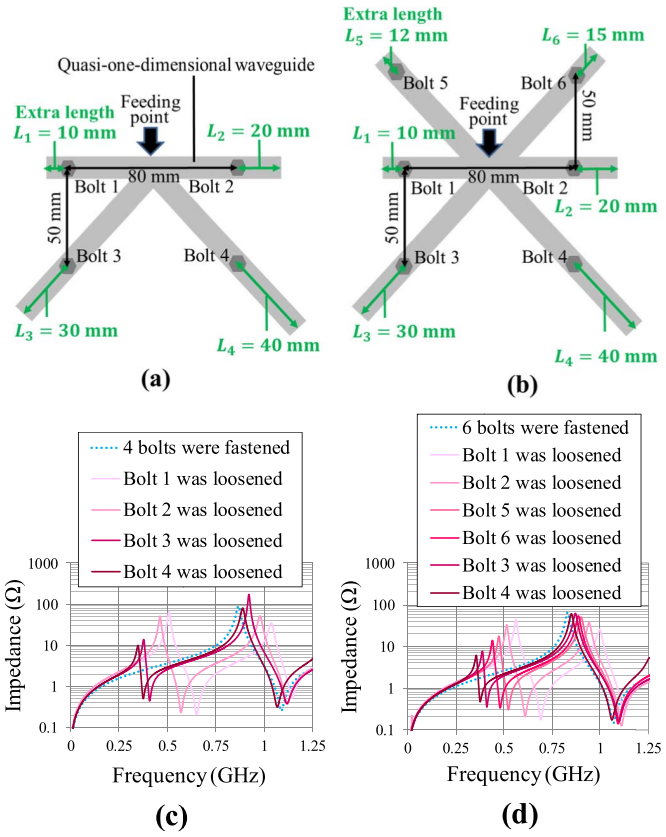

Fig. 13. Simulated frequency response of impedance when sensor monitors multiple bolts. (a) Design of sensor with 4 bolts installed; (b) Design of sensor with 6 bolts installed; (c) Simulated frequency response of impedance in the case of 4 bolts; (d) Simulated frequency response of impedance in the case of 6 bolts.

similar sensitivity even when the number of bolts to be monitored increases, because the minimum detection angle is comparable to that of the single-detection sensor.

Furthermore, we designed and simulated sensors for monitoring 4 or 6 bolts, as shown in Fig. 13 (a) and (b). The extra lengths of the bolts were varied and the loose bolts were identified. The simulated frequency responses are shown in Fig. 13 (c) and (d). The feeding point was placed at the center between bolt I and II. When a bolt was loosened, resonance peaks appeared between 0.3 to 0.6 GHz. Because of the difference between the extra lengths of the individual bolts, the resonance frequencies were also different. We could identify the loose bolts from the resonance frequencies. Note that while we can fabricate a sensor that can monitor an even larger number of bolts (i.e., more than 8), there will come a point when the number of bolts is too large and the difference in resonance frequency will be too small. Therefore, paintable two-dimensional sensor [21] is a good candidate for a sensor capable of monitoring many bolts.

V. Conclusion

In this paper, we demonstrated that multiple bolt loosening can be monitored with a single passive sensor that is fabricated by painting it directly on the structure. We proposed the principle of operation of this waveguide-based sensor in which resonance occurs due to a difference in waveguide resonance length. It was clearly demonstrated that the fabricated sensor can detect a loose bolt from resonance frequency changes in the sensor caused by abnormality-induced changes in the waveguide resonance. We also demonstrated that the loosening of multiple bolts can be monitored with a single sensor by controlling the resonance frequency by the difference in the extra length when a bolt is loosened. The concept behind this sensor is a new one and it should make remote inspection of infrastructure more efficient. We will study the durability of the sensor and the effects of the external environment in the future.

Acknowledgment

The authors are sincerely grateful to Ms. Emiko Konno for support with the sensor fabrication. They also thank Masahito Nakamura of NTT Device Technology Labs, NTT Corporation for helpful discussions about this study.

References

[1] Y. Fujino and D. M. Siringoringo, "Structural health monitoring of bridges in Japan: An overview of the current trend," in *Proc. 4th Int. Conf. FRP Compos. Civil Eng. (CICE)*, Zürich, Switzerland, Jul. 2008, pp. 1–12.

[2] M. Kušar and J. Šelih, "Analysis of bridge condition on state network in Slovenia," *Gradevinar*, vol. 66, no. 9, pp. 811–822, 2014.

[3] H. Fujii, A. Yamashita, and H. Asama, "Automated diagnosis of material condition in hammering test using a boosting algorithm," in *Proc. IEEE Int. Workshop Adv. Robot. Social Impacts*, Evanston, IL, USA, Sep. 2014, pp. 101–107.

[4] K. P. Chong, N. J. Carino, and G. Washer, "Health monitoring of civil infrastructures," *Smart Mater. Struct.*, vol. 12, no. 3, pp. 483–493, May 2003.

[5] B. Phares, Y. S. Lee, T. Brockman, and J. Rooney, "Investigation of high-strength bolt-tightening verification techniques," Digit. Repository, Iowa State Univ., Ames, IA, USA, Tech. Rep. InTrans Project 14-501, Iowa DOT Project SPR RB07-014, Mar. 2016.

[6] Q. Pan, R. Pan, C. Shao, M. Chang, and X. Xu, "Research review of principles and methods for ultrasonic measurement of axial stress in bolts," *Chin. J. Mech. Eng.*, vol. 33, no. 1, pp. 1–16, Feb. 2020, doi: 10.1186/s10033-020-0431-x.

[7] B. M. Phares, D. D. Rolander, B. A. Graybeal, and G. A. Washer, "Reliability of visual bridge inspection," *Public Roads*, vol. 64, no. 5, pp. 22–29, 2001.

[8] D. J. Pines and P. A. Lovell, "Conceptual framework of a remote wireless health monitoring system for large civil structures," *Smart Mater. Struct.*, vol. 7, no. 5, pp. 627–636, Oct. 1998.

[9] A. Ozden, A. Faghri, M. Li, and K. Tabrizi, "Evaluation of synthetic aperture radar satellite remote sensing for pavement and infrastructure monitoring," *Proc. Eng.*, vol. 145, pp. 752–759, Jan. 2016.

[10] K. Shuntaro, D. Hirotsugu, S. Masahiro, K. Nobuaki, and K. Toshio, "Investigation of the tunnel ceiling collapse in the central expressway in Japan," in *Proc. Transp. Res. Board 93rd Annu. Meeting*, Washington, DC, USA, 2014, p. 11.
[11] S. Narayanan, "I-35W Mississippi river bridge failure—Is it a wake up call?" *Indian Concrete J.*, vol. 19, no. 9, pp. 29–38, Feb. 2008.
[12] D. B. Cleary, W. T. Riddell, and C. J. Lacke, "Effect of washer placement on performance of direct tension indicators with curved protrusions," *Eng. J.*, vol. 49, no. 2, pp. 55–64, 2012.
[13] C. Popenoe, "Tension indicating fasteners," *Amer. Fastener J.*, vol. 20, pp. 1–3, May/Jun. 2011. Accessed: Apr. 9, 2021. [Online]. Available: http://www.smartbolts.com/wp-content/uploads/2011/04/SII_MayJune2011.pdf
[14] J. Shao, T. Wang, H. Yin, D. Yang, and Y. Li, "Bolt looseness detection based on piezoelectric impedance frequency shift," *Appl. Sci.*, vol. 6, no. 10, pp. 298–308, 2016.
[15] L. Huo, D. Chen, Q. Kong, H. Li, and G. Song, "Smart washer—A piezoceramic-based transducer to monitor looseness of bolted connection," *Smart Mater. Struct.*, vol. 26, no. 2, Feb. 2017, Art. no. 025033. Accessed: Apr. 8, 2021.
[16] X. Kong and J. Li, "Image registration-based bolt loosening detection of steel joints," *Sensors*, vol. 18, no. 4, pp. 1000–1020, 2018.
[17] J. H. Park, T. H. Kim, K. S. Lee, T. C. Nguyen, and J. T. Kim, "Novel bolt-loosening detection technique using image processing for bolt joints in steel bridges," ASEM, Incheon, South Korea, Lect. Note MS581_2517F1, 2015.
[18] K. Rokugo, H. Hatano, and Y. Mizobe, "Periodic inspection of PC bridge with both robot technologies and close visual observation," in *Proc. ConMat*, Fukuoka, Japan, 2020, pp. 1376–1384.
[19] S. Mekid, A. Bouhraoua, and U. Baroudi, "Battery-less wireless remote bolt tension monitoring system," *Mech. Syst. Signal Process.*, vol. 128, pp. 572–587, Aug. 2019.
[20] N. Hoult *et al.*, "Wireless sensor networks: Creating 'smart infrastructure,'" *Proc. ICE-Civil Eng.*, vol. 162, no. 3, pp. 136–143, Aug. 2009.
[21] E. Matsunaga, T. Minotani, S. Oka, and M. Tsuda, "Fundamental study of coating-type sensor for detection of infrastructure deterioration," in *Proc. 65th Jpn. Conf. Mater. Environ.*, Toyama, Japan, 2018, pp. 349–350.
[22] E. Matsunaga, M. Nakamura, T. Minotani, and M. Tsuda, "Paintable wireless passive sensor based on electromagnetic waveguide to detect loose bolts for remote infrastructure inspection," in *Proc. IEEE SENSORS*, Montreal, QC, Canada, Oct. 2019, pp. 1–4, doi: 10.1109/SENSORS43011.2019.8956933.
[23] W. Su, B. Cook, M. Tentzeris, C. Mariotti, and L. Roselli, "A novel inkjet-printed microfluidic tunable coplanar patch antenna," in *Proc. IEEE APSURSI*, Memphis, TN, USA, Jul. 2014, pp. 858–859.
[24] S. M. Bidoki, J. Nouri, and A. A. Heidari, "Inkjet deposited circuit components," *J. Micromech. Microeng.*, vol. 20, no. 5, May 2010, Art. no. 055023.
[25] L. G. Maloratsky and M. Lines, "Reviewing the basics of microstrip," *Microw. RF*, vol. 39, pp. 79–88, Mar. 2020.
[26] S. Aiswarya, M. Ranjith, and S. K. Menon, "Passive RFID tag with multiple resonators for object tracking," in *Proc. PIERS-FALL*, Singapore, Nov. 2017, pp. 742–746.
[27] A. Eroglu, "High-power transmission line transformer design for plasma generators," *IEEE Trans. Plasma Sci.*, vol. 42, no. 4, pp. 969–975, Apr. 2014.
[28] K. Zhao and L. E. R. Petersson, "Overview of hybrid solver in HFSS," in *Proc. IEEE Int. Symp. Antennas Propag. USNC/URSI Nat. Radio Sci. Meeting*, Boston, MA, USA, Jul. 2018, pp. 411–412.
[29] S. Fujii, S. Kawamura, D. Mochizuki, M. M. Maitani, E. Suzuki, and Y. Wada, "Microwave sintering of Ag-nanoparticle thin films on a polyimide substrate," *AIP Adv.*, vol. 5, no. 12, Dec. 2015, Art. no. 127226, doi: 10.1063/1.4939095.
[30] S. Y. Huang *et al.*, "Microstrip line-based glucose sensor for noninvasive continuous monitoring using the main field for sensing and multivariable crosschecking," *IEEE Sensors J.*, vol. 19, no. 2, pp. 535–547, Jan. 2019.
[31] *Tohnichi Torque Handbook*, Tohnichi Manuf., Tokyo, Japan, 2014, vol. 8, pp. 36–37.

Eri Matsunaga received the B.E. and M.E. degrees from Waseda University, Tokyo, Japan, in 2010, and 2012, respectively.

In April 2012, she joined NTT Energy and Environment Systems Laboratories, Atsugi, Kanagawa, Japan, where she worked on development of materials for lithium-ion batteries and resource visualization technology. Since 2015, she has been with NTT Device Technology Laboratories, Atsugi, where she is working on the development of technology to visualize deterioration of infrastructure.

Tadashi Minotani (Member, IEEE) received the B.S., M.S., and Ph.D. degrees in electronic engineering from Kyushu University, Fukuoka, Japan, in 1995, 1997, and 2000, respectively. In 2000, he joined the NTT Telecommunications Energy Laboratories (now the NTT Device Technology Laboratories), Kanagawa, Japan. He received the 2002 Asia Pacific Microwave Conference APMC Prize. He is a member of IECE.

Masayuki Tsuda received the M.E. and Dr.Eng. degrees in mechanical engineering from the Tokyo Institute of Technology in 1998 and 2005, respectively. He joined NTT Integrated Information and Energy Systems Laboratories in 1998, where he worked on the development of materials for lithium-ion batteries and environmental impact assessment of ICT services. From 2013 to 2018, he worked with the NTT Environment Promotion Office. Since 2018, he has been with NTT Device Technology Laboratories, where he is working on the development of technology to visualize deterioration of infrastructure.